Molecular Pharmacology Fast Forward. Published on August 31, 2011 as doi:10.1124/mol.111.074674

MOL #74674

TITLE PAGE

Developing chemical genetic approaches to explore G protein-coupled receptor function – Validation of the use of a receptor activated solely by synthetic ligand (RASSL)

Elisa Alvarez-Curto, Rudi Prihandoko, Christofer S. Tautermann, Jurriaan M. Zwier, John D. Pediani, Martin J. Lohse, Carsten Hoffmann, Andrew B. Tobin and Graeme Milligan

Molecular Pharmacology Group, Institute of Neuroscience and Psychology, College of Medical, Veterinary and Life Sciences, University of Glasgow, Glasgow G12 8QQ, Scotland U.K. (EA-C, JDP, GM), Department of Cell Physiology and Pharmacology, University of Leicester, Hodgkin Building, Lancaster Road, Leicester LE1 9HN, England, U.K. (RP, ABT), Boehringer Ingelheim Pharma GmbH & Co. KG, Lead Identification and Optimization Support, 88397 Biberach, Germany (CST), Cisbio Bioassays, Parc Marcel Boiteux, BP84175, 30200 Codolet, France (JMZ), Department of Pharmacology and Toxicology, University of Wuerzburg, Versbacher Str. 9, 97078 Wuerzburg, Germany (MJL,CH)

Molecular Pharmacology Fast Forward. Published on August 31, 2011 as DOI: 10.1124/mol.111.074674
This article has not been copyedited and formatted. The final version may differ from this version.

MOL #74674

RUNNING TITLE PAGE

Running title: Muscarinic RASSL function

Corresponding author: Graeme Milligan, Wolfson Link Building 253, University of Glasgow,Glasgow G12 8QQ, Scotland, U.K.

Tel +44 141 330 5557, FAX +44 141 330 5481

e-mail: Graeme.Milligan@glasgow.ac.uk

Manuscript information:

Number of text pages: 44

Number of figures: 10

Number of tables: 1

Number of references: 42

Number of words in Abstract: 250

Number of words in Introduction: 533

Number of words in Discussion: 1575

Non-standard abbreviations: DREADD, Designer Receptor Exclusively Activated by Designer Drugs; FlAsH, fluorescein arsenical hairpin binder; GPCR, G protein-coupled receptor; IL3, third intracellular loop; QNB, quinuclidinyl benzilate; RASSL, Receptor Activated Solely by Synthetic Ligand

Molecular Pharmacology Fast Forward. Published on August 31, 2011 as DOI: 10.1124/mol.111.074674
This article has not been copyedited and formatted. The final version may differ from this version.

ABSTRACT

Molecular evolution and chemical genetics have been applied to generate functional pairings of mutated G protein-coupled receptors and non-endogenous ligands. These mutant receptors, referred to as RASSL or DREADD receptors, have huge potential to define physiological roles of GPCRs and to validate receptors in animal models as therapeutic targets to treat human disease. However, appreciation of ligand bias and functional selectivity of different ligands at the same receptor suggests that RASSLs may signal differently than wild type receptors activated by endogenous agonists. We assessed this by generating forms of wild type human M_3 muscarinic receptor and a RASSL variant that responds selectively to clozapine N-oxide. Although the RASSL receptor had reduced affinity for muscarinic antagonists, including atropine, stimulation with clozapine N-oxide produced very similar effects as those generated by acetylcholine at the wild type M_3-receptor. Such effects included the relative movement of the third intracellular loop and C-terminal tail of intramolecular FRET sensors and the ability of the wild type and evolved mutant to regulate ERK1/2 phosphorylation. Each form interacted similarly with β-arrestin 2 and was internalized from the cell surface in response to the appropriate ligand. Furthermore, the pattern of phosphorylation of specific serine residues within the evolved receptor in response to clozapine N-oxide was very similar to that produced by acetylcholine at the wild type. Such results provide confidence that, at least for the M_3 muscarinic receptor, results obtained following transgenic expression of this RASSL are likely to mirror the actions of acetylcholine at the wild type receptor.

Molecular Pharmacology Fast Forward. Published on August 31, 2011 as DOI: 10.1124/mol.111.074674
This article has not been copyedited and formatted. The final version may differ from this version.

INTRODUCTION

In recent times a number of G protein-coupled receptors (GPCRs) have been modified such that they become able to respond to a previously inert synthetic ligand whilst, in parallel, they lose the ability to be activated by their native, endogenously produced ligand(s) (Conklin et al., 2008, Pei et al., 2008, Dong et al., 2010). Such modified receptors are described as either Receptors Activated Solely by Synthetic Ligands (RASSLs) or as Designer Receptors Exclusively Activated by Designer Drugs (DREADDs) (Conklin et al., 2008, Pei et al., 2008, Dong et al., 2010). Such variants have been expressed transgenically to explore specific functions of the parent receptor when the synthetic ligand is provided (Guettier et al., 2009, Sweger et al., 2007, Redfern et al., 2009, Alexander et al, 2009). This approach has been of particular value in examples, such as the muscarinic acetylcholine receptors, where each of the five native muscarinic receptor subtypes responds to acetylcholine with similar potency (Guettier et al., 2009, Alexander et al., 2009, Armbruster et al., 2007, Nawaratne et al., 2008). Furthermore, identification of pharmacological agents that interact at a binding site that overlaps with that of acetylcholine, but with high selectivity for an individual subtype has been difficult to achieve (Digby et al., 2010, Conn et al., 2009).

It is now widely appreciated that subtle modifications in agonist ligand structure can result in stabilization of distinct active states of a GPCR (Bhattacharya et al., 2008, Swaminath et al., 2005, Kobilka and Deupi, 2007). Such individual states can differentially modulate cellular signalling pathways (Bhattacharya et al., 2008, Swaminath et al., 2005, Kobilka and Deupi, 2007) and, therefore, there must be a concern that use of a combination of a modified receptor and a distinct ligand might result in different outputs and, hence, compromise the utility of such pairings to define details of function of the native receptor *in vivo*. There is already some

Molecular Pharmacology Fast Forward. Published on August 31, 2011 as DOI: 10.1124/mol.111.074674
This article has not been copyedited and formatted. The final version may differ from this version.

evidence to favor this suggestion from studies performed on the serotonin 5-HT_4 receptor (Chang et al., 2007). This issue has not, however, been addressed previously in any detail. Using various forms of the wild type human muscarinic M_3 receptor in parallel with equivalent RASSL forms of this receptor modified to respond to clozapine N-oxide rather than acetylcholine, we have explored potential differences at varying levels of receptor and cellular response. Perhaps surprisingly, whether exploring initial conformational changes that occur upon ligand binding, interactions with β-arrestin 2, receptor internalization, ligand-induced phosphorylation of the ERK1/2 MAP kinases or the extent and profile of phosphorylation of the receptor in response to appropriate agonists, the pattern of regulation was very similar for the wild type and RASSL forms. This is despite a large reduction in affinity of the RASSL to bind the well characterized muscarinic receptor antagonist [^{3}H]QNB and the widely used anti-muscarinic drug atropine. Molecular modelling provided a rationale for the selective activation of the RASSL variant by the selective ligand. These studies provide a strong indication that, at least for the M_3 receptor, this modified version is likely to allow production of meaningful and relevant information when expressed transgenically. Furthermore, they reinforce the use of designer receptors as valid and powerful tools to define and understand physiological responses in animal models.

MATERIALS AND METHODS

Materials – Materials for cell culture were from Sigma-Aldrich (Gillingham, UK) or Invitrogen (Paisley, UK). Clozapine-N-oxide was from Enzo Life Sciences Ltd. (Exeter, UK). Other drugs used in this study were from Sigma-Aldrich (Gillingham, UK). The various anti-muscarinic M_3-R antibodies and phospho-serine site-specific antisera have been described previously (Poulin et al., 2010, Butcher et al., 2011,

Molecular Pharmacology Fast Forward. Published on August 31, 2011 as DOI: 10.1124/mol.111.074674
This article has not been copyedited and formatted. The final version may differ from this version.

Torrecilla et al., 2007). All secondary IgG horseradish peroxidase linked antibodies were from GE Healthcare (Amersham, UK). The radioligand [^{3}H]QNB was from Perkin Elmer (Boston, MA). All oligonucleotides were purchased from ThermoElectron (Ulm, Germany). Flp-In™ T-REx™ 293 cells were from Invitrogen (Paisley, UK). Tag-lite® reagents and SNAP-tag reagents were supplied by Cisbio Bioassays, (Bagnols sur Ceze, France) and New England Biolabs (Hitchin, UK).

Molecular constructs

Generation of the human muscarinic M_3 (hM_3)-RASSL by site-directed mutagenesis and VSV-G-SNAP-hM_3-R and VSV-G-SNAP-hM_3-RASSL constructs was described previously (Alvarez-Curto et al., 2010). The hM_3-R intramolecular FRET-sensor construct was generated as described in Ziegler *et al*. (2011). Briefly, the short amino acid motif CCPGCC which specifically defines the fluorescein arsenical hairpin binder (FlAsH) sequence was introduced as replacement of amino acids 271 to 465 in the third intracellular loop (IL3) of the hM_3-R. The modified receptor was then fused in-frame to a variant of the cyan fluorescent protein (eCFP) (BD Bioscience Clontech, Heidelberg, Germany). All resulting constructs were cloned into either pcDNA3 or pcDNA5/FRT/TO (Invitrogen) and confirmed by sequencing. The equivalent hM_3-RASSL intramolecular FRET-sensors introduced either or both cysteine (C) for tyrosine (Y) at residue 149 (position 3.33 in the nomenclature of Ballesteros and Weinstein (1995)) and glycine (G) for alanine (A) at residue 239 (position 5.46) as described previously (Armbruster et al., 2007).

Generation of stable Flp-In™ T-REx™ 293 cells

Cells were maintained in Dulbecco's modification of Eagle's medium (DMEM) without sodium pyruvate, 4500 mg/liter glucose, and L-glutamine, supplemented with 10%

Molecular Pharmacology Fast Forward. Published on August 31, 2011 as DOI: 10.1124/mol.111.074674
This article has not been copyedited and formatted. The final version may differ from this version.

(v/v) fetal calf serum, 1 % penicillin/streptomycin mixture, and 10 $\mu g.ml^{-1}$ blasticidin in a humidified atmosphere. To generate Flp-In™ T-REx™ 293 cells able to inducibly express the different cDNA constructs, cells were transfected with a 1:9 mixture of cDNA in pcDNA5/FRT/TO vector and the pOG44 vector (Invitrogen) using Effectene (Qiagen, West Sussex, UK), according to the manufacturer's instructions and as described previously (Ward et al., 2011, Smith et al., 2009., Stoddart et al., 2008, Ellis et al., 2006). After 48 h, the medium was changed to medium supplemented with 200 $\mu g.ml^{-1}$ hygromycin B (Roche Diagnostics, Mannheim, Germany) to initiate selection of stably transfected cells.

Cell membrane preparation

Pellets of cells were frozen at -80^{o}C for a minimum of 1 h, thawed and resuspended in ice-cold 10 mM Tris, 0.1 mM EDTA, pH 7.4 (TE buffer) supplemented with Complete protease inhibitors cocktail (Roche Diagnostics). Cells were homogenized on ice by 40 strokes of a glass-on-Teflon homogenizer followed by centrifugation at 1000 x g for 5 min at 4°C to remove unbroken cells and nuclei. The supernatant fraction was removed and passed through a 25-gauge needle 10 times before being transferred to ultracentrifuge tubes and subjected to centrifugation at 50,000 x g for 45 min at 4°C. The resulting pellets were resuspended in ice-cold TE buffer. Protein concentration was assessed and membranes were stored at -80°C until required.

Radioligand binding assays

Saturation binding isotherms were established following the addition of 1 µg (hM_3-R) or 10 µg (hM_3-RASSL) of membrane protein to assay buffer (20 mM HEPES, 100 mM NaCl, and 10 mM $MgCl_2$, pH 7.4) containing varying concentrations of [^{3}H]QNB (50.5 Ci/mmol). Non-specific binding was determined in the presence of 10 µM

Molecular Pharmacology Fast Forward. Published on August 31, 2011 as DOI: 10.1124/mol.111.074674
This article has not been copyedited and formatted. The final version may differ from this version.

atropine. Reactions were incubated for 90 min at 30^{o}C, and bound ligand was separated from free by vacuum filtration through GF/C filters (Brandel Inc., Gaithersburg, MD). The filters were washed twice with assay buffer, and bound ligand was estimated by liquid scintillation spectrometry.

Cell lysates and Western blotting

Cells were washed once in cold phosphate buffered saline (PBS) and harvested with ice-cold radioimmune precipitation (RIPA) buffer (50 mM HEPES, 150 mM NaCl, 1% Triton X-100, and 0.5% sodium deoxycholate, 10 mM NaF, 5 mM EDTA, 10 mM NaH_2PO_4, 5% ethylene glycol, pH 7.4) supplemented with Complete protease inhibitors cocktail (Roche Diagnostics). Extracts were passed though a 25-gauge needle and incubated for 15 min at 4^{o}C while spinning on a rotating wheel. Cellular extracts were then centrifuged for 30 min at 14000 x g and the supernatant was recovered. Samples were heated at 65^{o}C for 15 min and subjected to SDS-PAGE analysis using 4–12% BisTris gels (NuPAGE, Invitrogen) and MOPS buffer. Proteins were then electrophoretically transferred onto nitrocellulose membranes that were blocked for 45 min in 5 % fat-free milk in TBST (1 x Tris Buffered Saline) containing 0.1 % (v/v) Tween 20) and subsequently incubated with the required primary antibody overnight at 4^{o}C. Incubation with the appropriated horseradish peroxidase-linked IgG secondary antiserum was performed for 2h at room temperature. Immunoblots were developed by application of enhanced chemiluminescence solution (Pierce).

ERK1/2 phosphorylation assays

ERK1/2 phosphorylation assays were performed using the AlphaScreen® Surefire® kit (PerkinElmer, Amersham, UK). Cells were plated on 96 well poly-D-lysine-coated

Molecular Pharmacology Fast Forward. Published on August 31, 2011 as DOI: 10.1124/mol.111.074674
This article has not been copyedited and formatted. The final version may differ from this version.

plates (40,000 cells/well) and receptor construct expression induced the next day with either varying concentrations or 5 $ng.ml^{-1}$ doxycycline. In experiments where pertussis toxin was used, 25 $ng.ml^{-1}$ was added simultaneously with the doxycycline and incubated for 16-18 h. Before ligand stimulation, cells were serum-starved for 5 h in growth medium lacking FBS. Stimulation of cells was terminated by rapid aspiration of the medium and fast addition of 50 µl of 1x lysis buffer that is provided with the kit. Lysates were subsequently processed according to the manufacturer's instructions.

$[Ca^{2+}]_i$ mobilization assays

Cells induced to express forms of either hM_3-R or hM_3-RASSL were plated in clear-bottom black 96 well plates (Greiner) and induced with 5 $ng.ml^{-1}$ of doxycycline for 24 h. Cells were incubated at 37^oC in the dark with the Ca^{2+} sensitive dye Fura-2 diluted to 3 µM in DMEM for 30 min, subsequently washed twice with HEPES physiological saline solution (130 mM NaCl, 5 mM KCl, 1 mM $CaCl_2$, 1 mM $MgCl_2$, 20 mM HEPES, and 10 mM D-glucose, pH 7.4) and transferred to a FlexStation II (Molecular Devices, Sunnydale, CA) where they were treated with ligands. Alteration of intracellular calcium was recorded as changes of Fura-2 340/380 nm emission ratio.

Tag-lite® internalization assays

Cells were plated on black, poly-D-lysine coated 96 well plates (100,000 cells/well), and induced with 5 $ng.ml^{-1}$ of doxycycline for 24 h. Next day the plate was cooled on ice for 5 min and cells were labelled with 100 nM SNAP-Lumi4Tb for 1 h at 4^oC. Cells were washed four times with cold labelling medium (Cisbio Bioassays), after which ligands and Tag-lite® internalization buffer were added. Plates were then read at different time intervals in a PheraStar FS (BMG Labtechologies, Offenburgh,

Molecular Pharmacology Fast Forward. Published on August 31, 2011 as DOI: 10.1124/mol.111.074674
This article has not been copyedited and formatted. The final version may differ from this version.

Germany) plate reader, monitoring the changes of donor emission at 620 nm (integration start = 1500 µs; integration time = 1500 µs) and acceptor emission at 520 nm (integration start = 150 µs; integration time = 400 µs). The ratio was finally calculated as (donor / acceptor channel) * 10000.

β-arrestin-2 BRET assays

HEK293T cells were transfected with the required receptor C-terminally tagged with mCitrine and β-arrestin-2 C-terminally tagged with *Renilla* luciferase 8 (Rluc) (ratio 4:1), using polyethyleneimine (Jenkins et al., 2010, 2011). An additional transfection was performed with only the *Renilla* luciferase (Rluc) construct and empty expression vector pcDNA3. From 10 cm dishes, cells were seeded at 50,000 cells per well into poly-D-lysine coated white 96 well plates. After 24 h, cells were washed twice with Hank's Balanced Salt Solution (pH 7.4), and coelentrazine-h (Promega, Southampton, UK) was added to a final concentration of 5 µM. Cells were incubated in darkness for 10 min at 37°C before addition of ligands after what they were incubated for a further 10 min at 37°C before reading on a PheraStar FS plate reader (BMG, Germany), that allows simultaneous reading of emission signals detected at 475 nm and 535 nm. Net BRET values were defined as the 535 nm/475 nm ratio of cells co-expressing Rluc and mCitrine minus the BRET ratio of cells expressing only the Rluc construct in the same experiment. This value was multiplied by 1000 to obtain mBRET units.

Epifluorescence imaging of SNAP-tag proteins in live cells

Cells induced to express the receptor construct of interest were grown on coverslips pre-treated with 0.1 $mg.ml^{-1}$ poly-D-lysine. SNAP-tag specific substrates were diluted in complete DMEM medium from a stock solution yielding a labelling solution of 5 µM

Molecular Pharmacology Fast Forward. Published on August 31, 2011 as DOI: 10.1124/mol.111.074674
This article has not been copyedited and formatted. The final version may differ from this version.

dye substrate. The medium on the cells expressing a SNAP-tag fusion protein was replaced with the labelling solution and incubated at 37°C, 5% CO_2 for 30 min. Cells were washed three times with complete medium and a further time with HEPES physiological saline solution (130 mM NaCl, 5 mM KCl, 1 mM $CaCl_2$, 1 mM $MgCl_2$, 20 mM HEPES, and 10 mM D-glucose, pH 7.4). Coverslips were then transferred to a microscope chamber where they were imaged using an inverted Nikon TE2000-E microscope (Nikon Instruments, Melville, NY) equipped with a 40x (numerical aperture-1.3) oil-immersion Pan Fluor lens and a cooled digital photometrics Cool Snap-HQ charge-coupled device camera (Roper Scientific, Trenton, NJ).

FlAsH labelling

Cells were grown on poly-D-lysine-treated glass coverslips (number 0) and induced to express the construct of interest with doxycycline for 24 h. The next day the coverslips bearing induced cells were transferred to 6-well multiplates containing 2 ml of control phenol red-free Hank's balanced salt solution, (HBSS), 1x supplemented with 10 mM Glucose (Invitrogen, catalog no. 14025-050). Each well was washed three times (10 min per wash) with control HBSS. After the final wash, the HBSS solution was aspirated from each well and replaced with 1.8 ml of control HBSS. In between washes, HBSS containing 1 µM FIAsH and 12.5 µM ethanedithiol (EDT) was prepared fresh as follows: 1) 25 mM EDT DMSO solution was freshly prepared in a 2 ml Eppendorf tube by adding. 2) 2.1 µl of EDT to 1 ml of DMSO and then vortex mixed. This mixture was at room temperature for 20 min to ensure complete conversion of FIAsH to its FIAsH-EDT2 form. 1 µM FIAsH labelling solution, (for six coverslip samples), was made by firstly adding 6 µl of 2 mM lumiogreen stock solution, (Invitrogen), to a new 2 ml Eppendorf tube. 6 µl of 25 mM EDT was then added to this solution, mixed and left in the dark at room temperature for 20 min. 3)

Molecular Pharmacology Fast Forward. Published on August 31, 2011 as DOI: 10.1124/mol.111.074674
This article has not been copyedited and formatted. The final version may differ from this version.

After 20 min, 1.2 ml of control HBSS solution containing 10 mM glucose was added to this tube and vortex mixed. This EDT/FlAsH/HBSS solution was then allowed to stand for 20 min in the dark to ensure complete binding of EDT. 4) After 20 min, 200 µl amounts of the EDT/FlAsH/HBSS solution were added to each well containing 1.8 ml of control HBSS. The 6 well multiplate was then gently swirled to ensure uniform distribution of the labelling solution. Cells were then incubated at 37°C for 1 h in the dark with the FlAsH suspended HBSS solution containing 12.5 µM EDT. During this incubation period EDT/HBSS washing solution was prepared by mixing 42 µl of EDT with 1 ml of DMSO in a 1.5 ml Eppendorf tube, (500 mM EDT in DMSO). 25 µl of this mixture was added to 50 ml of control HBSS and mixed to form a final HBSS/glucose solution containing 250 µM EDT. After 1 h, the cells were removed from the incubator and the FlAsH labelling solution was then aspirated from each well and replaced with 3 ml of EDT/HBSS wash solution. Cells were incubated for 15 min in the dark to reduce non-specifically bound FlAsH. This washing procedure was repeated twice more to further reduce background staining. Cells were then rinsed three times, (5 minutes/wash), with FlAsH-free control HBSS solution to ensure complete removal of EDT from labelled cells. Labelled cells were then stored at room temperature in the dark prior to intramolecular fluorescence resonance energy transfer (FRET) imaging experimentation.

Intramolecular eCFP-FlAsH FRET experiments

Washed FlAsH-labeled cells were placed into a microscope chamber containing physiological HEPES-buffered saline solution (130 mM NaCl, 5 mM KCl, 1 mM $CaCl_2$, 1 mM $MgCl_2$, 20 mM HEPES, and 10 mM D-glucose, pH 7.4). Cells were then imaged using an inverted Nikon TE2000-E microscope (Nikon Instruments) equipped with a ×40 (numerical aperture = 1.3) oil immersion Fluor lens. Excitation light was

Molecular Pharmacology Fast Forward. Published on August 31, 2011 as DOI: 10.1124/mol.111.074674
This article has not been copyedited and formatted. The final version may differ from this version.

generated from a computer-controlled Optoscan monochromator (Cairn Research, Faversham, UK), which was coupled to an ultra-highpoint intensity Optosource lamp, (Cairn Research), fitted with a 103 watt mercury arc lamp (Osram 103W/2). Monochromator was set to 427 nm/band width, (BW) 5 nm or 504nm/BW 5 nm, to visualize surface located eCFP-tagged receptors labeled with FlAsH. Excitation light, (427 nm or 504 nm), was reflected through the Fluor objective lens using a cyan/yellow fluorescent protein dual band dichroic filter (Semrock; Rochester, NY, catalog no. FF440/520-Di01), mounted in the microscope. FRET and donor emission images were recorded exactly at the same time interval using a Quadview 2, (QV2), image splitting device, (Photometrics, UK), coupled to a CoolSnap-HQ2 camera connected to the microscope's bottom port for maximal detection of emitted fluorescence. FRET and donor signals were detected simultaneously using the following Chroma (Chroma, Brattleboro, VT), ET series dichroic and emitters mounted in the QV2 cube: ET t505LPXR dichroic, ET535/30 nm, ET 470/30 nm.

Using the streaming capability of the multiple dimensional wavelength acquisition module of MetaMorph, ligand induced changes in intramolecular FRET were recorded at 40 ms intervals during excitation with 427 nm light directly to the computer's hard drive. The Cool Snap-HQ2 camera was operated in 14-bit mode and exposure time, binning (8 × 8), and camera gain, were kept constant for all streaming experiments. Computer control of all electronic hardware and camera streaming acquisition was achieved using Metamorph software (version 7.7.4 Molecular Devices, Sunnydale, CA). TTL controlled solenoid valves connected to a peristaltic pump operated at a flow rate of 5 ml/min were used to rapidly add or remove test ligand drugs into the imaging chamber.

Intramolecular FRET ratio quantification

Molecular Pharmacology Fast Forward. Published on August 31, 2011 as DOI: 10.1124/mol.111.074674
This article has not been copyedited and formatted. The final version may differ from this version.

Using Metamorph's split view module, saved images were split to form individual FRET or donor stream time-lapse stacks. Each stack was corrected for background fluorescence and exported into Metamorph's align module to ensure there was no x or y pixel shift misalignment between the donor and FRET channel stream stacks prior to the calculation of the intramolecular FRET ratio. Intramolecular FRET values were measured by manually drawing regions of interest, (ROI), around the profile of individual cells and averaging the signals within the delimited ROI for each time-lapse image collected at 470 or 535 nm emission. Ratiometric FRET values were then calculated as the average 535 nm emission intensity divided by the average 470 nm emission intensity. Quantified ratio values were exported into Prism 5.02 (GraphPad Software Inc.) and using Graphpad's transforming module set to a value of 1.0 at the onset of each experiment and plotted over time.

[^{32}P]-orthophosphate labelling and hM$_3$ receptor immunoprecipitation

Cells grown on 6-well plates at ~ 90% confluence were washed three times in 1 ml phosphate free Krebs/HEPES buffer (10 mM HEPES, 118 mM NaCl, 4.69 mM KCl, 1.18 mM $MgSO_4.7H_2O$, 1.3 mM $CaCl_2$, 25.0 mM $NaHCO_3$, 11.7 mM glucose, pH 7.4) and then incubated with 50 µCi/ml [^{32}P]-orthophosphate (PerkinElmer, 185 MBq) for 1 h at 37^{o}C. Cells were stimulated with the appropriate agonist for 5 min at 37^{o}C. The reactions were terminated by rapid aspiration of the buffer followed by addition of 1 ml ice-cold radio-immunoprecipitation (RIPA) buffer (10 mM Tris, 160 mM NaCl, 2 mM EDTA, 20 mM glycerol-2-phosphate, 1% Nonidet P-40, 0.5% sodium deoxycholate, pH 7.4) for 10 min on ice. Cell lysates were cleared by centrifugation (20 000 *g* for 5 min) and receptors were immunoprecipitated from pre-cleared lysates using 2 µg/sample of in-house polyclonal anti-M$_3$-Receptor antibody. Immunocomplexes were isolated on protein A-Sepharose beads (Fisher, 1.5 g) and

Molecular Pharmacology Fast Forward. Published on August 31, 2011 as DOI: 10.1124/mol.111.074674
This article has not been copyedited and formatted. The final version may differ from this version.

the beads were washed three times with ice-cold TEG buffer (10 mM Tris, 2 mM EDTA, 20 mM glycerol-2-phosphate, pH 7.4). Immunocomplexes were resuspended in 2x SDS-PAGE sample buffer (125 mM Tris, 200 mM dithiothreitol, 4% SDS, 20% glycerol and 0.05% bromophenol blue, pH 6.8) and placed in a 60^{o}C water bath for 3-5 min. Receptor proteins were resolved on 8% SDS-PAGE gels and electroblotted onto nitrocellulose membranes using the semi-dry transfer method (Bio-Rad) and Tris-glycine transfer buffer (25 mM Tris, 190 mM glycine, 20% methanol). Receptor phosphorylation was detected by autoradiography.

Tryptic digestion and 2-dimensional electrophoresis

Nitrocellulose membrane containing the receptor of interest was excised and incubated with 200 µl of blocking solution (0.5% PVP containing 0.6% acetic acid) for 30 min at 37^{o}C. Membrane pieces were washed three times with distilled water and one time with 50 mM ammonium bicarbonate. Proteins on the membrane pieces were digested with 10 µg.ml^{-1} trypsin (Promega) diluted in 50 mM ammonium bicarbonate solution overnight at 37^{o}C (60 µl final volume). The supernatant from the tryptic digest was recovered and transferred to fresh tubes. The membrane pieces were washed three times with 50-100 µl distilled water. The supernatant from each wash was pooled and dried using SpeedVac at room temperature for 2-6 h. The pellet was dissolved in 25-50 µl of pH 1.9 buffer (88% formic acid: acetic acid: water, 25:78:897 (v/v/v)) and dried again using the speedVac centrifuge. The pellet was resuspended in 5 – 10 µl of pH 1.9 buffer, vortex mixed intensely and applied to a cellulose thin layer chromatography plate in small volumes (≤ 1 µl). Samples were dried with a fan without heating and separated in two dimensions. The first dimension was electrophoresis in pH 1.9 buffer for 30-40 min at 2000 V using the HTLE 7002 electrophoresis system. The second dimension was ascending thin layer

Molecular Pharmacology Fast Forward. Published on August 31, 2011 as DOI: 10.1124/mol.111.074674
This article has not been copyedited and formatted. The final version may differ from this version.

chromatography using isobutyric acid chromatography buffer (isobutyric acid:n-butanol:pyridine:acetic acid:water, 1250:38:96:58:558 (v/v/v/v/v). The plate was dried extensively in a fume hood, wrapped in cling film and exposed to a phosphoimager. Resolved phosphopeptides were visualised using the STORM phosphoimager instrument (Amersham Biosciences) and quantified using alphaimager software.

RESULTS

Analysis of ligand-induced conformational changes in hM_3 intramolecular FRET sensors

Detailed analysis of the effects of ligands on rapid changes in conformation or activation state(s) of GPCRs can be performed using intramolecular FRET sensors (Hoffmann et al., 2005, Zurn et al., 2009). In initial studies we expressed transiently in HEK293T cells a form of the hM_3-R containing a fluorescein arsenical hairpin binder via tetra-cysteine (FlAsH) tag inserted into the third intracellular loop (IL3) and with enhanced cyan fluorescent protein (eCFP) linked in-frame to the C-terminal tail. To optimize the FRET response we deleted a large of a segment (amino acids 271-465) from IL3 (Ziegler et al., 2011). Once the FlAsH tag had been labelled with the FRET acceptor lumiogreen, this construct generated a rapid increase in the basal FRET signal upon addition of carbachol but not clozapine N-oxide (**Figure 1A**). We then introduced Y149C and/or A239G mutations into this construct both individually and in combination and repeated the studies. The sensor containing only the Y149C mutation responded to neither carbachol nor clozapine N-oxide (**Figure 1B**) whilst the sensor containing only the A239G mutation responded to carbachol (1 mM), although with slower kinetics than the hM_3–R sensor, but failed to respond to clozapine N-oxide (**Figure 1C**). Following introduction of both the Y149C and A239G alterations into the receptor sequence, the sensor did not respond to carbachol at

Molecular Pharmacology Fast Forward. Published on August 31, 2011 as DOI: 10.1124/mol.111.074674
This article has not been copyedited and formatted. The final version may differ from this version.

concentrations up to 1 mM but did respond to clozapine N-oxide, with a significantly larger response to 100 μM than to 10 μM of this ligand (**Figure 1D**). As such, it behaved as an hM_3-RASSL FRET sensor.

Based on these initial studies Flp-In™ T-REx™ 293 cell lines able to express either the hM_3-R or the hM_3-RASSL FRET sensor were generated. Here receptor expression is under the control of a doxycycline-inducible promoter. Saturation binding studies performed on membranes generated from cells induced to express the hM_3-R sensor showed this construct to have high affinity (K_D = 75 +/- 28 pM, mean +/- SEM, n=3) for [^{3}H]QNB (**Figure 2A**) whilst the hM_3-RASSL sensor displayed some 100 fold lower affinity for this ligand (K_D = 7.9 +/- 2.2 nM, mean +/- SEM, n=3) (**Figure 2B**), a feature that presumably reflects alteration of the amino acids used to create the RASSL within the ligand binding pocket of the hM_3-R (see Discussion). As atropine is frequently used as a standard muscarinic antagonist, and was used to define non-specific binding of [^{3}H]QNB in these studies, we also assessed the affinity of this ligand at these two forms of the hM_3 receptor via competition binding studies. Atropine also displayed reduced affinity at the hM_3-RASSL sensor (estimated K_i = 47 +/-17 nM; mean +/- SEM) compared to the equivalent hM_3-R (estimated K_i = 0.74 +/- 0.1 nM; mean +/- SEM).

We next assessed the functionality of the expressed constructs in calcium mobilization assays. Despite the multiple molecular modifications introduced into the receptors, each was able to respond robustly to the appropriate agonists, with potency for carbachol and acetylcholine in the case of the hM_3-R construct (pEC_{50} = 7.2 +/- 0.04 and 7.8 +/- 0.3; mean +/- SEM, n = 3, respectively) and to clozapine N-oxide at the hM_3-RASSL (pEC_{50} = 7.6 +/- 0.1; mean +/- SEM, n = 3) (**Figure 2C**, **Table 1**).

Molecular Pharmacology Fast Forward. Published on August 31, 2011 as DOI: 10.1124/mol.111.074674
This article has not been copyedited and formatted. The final version may differ from this version.

Following addition of the FlAsH labelling reagent lumiogreen to cells induced to express either of the intramolecular FRET sensors (**Figure 3A**) and subsequent washout, imaging of these cells showed the FlAsH sequence to be labelled effectively (**Figure 3B**). Parallel imaging also identified the presence of the eCFP tag at the surface of the cells (**Figure 3B**). FRET imaging of cells induced to express the hM_3-R FRET sensor demonstrated a rapid increase in FRET signal upon addition of acetylcholine but not in response to either clozapine N-oxide or atropine (not shown). Carbachol also induced a rapid and concentration-dependent increase in FRET (**Figure 3C, left**) with pD_2 = 4.9 +/- 0.2 (mean +/- SEM, n = 5)(**Table 1**). In cells expressing the hM_3-RASSL sensor clozapine N-oxide (pD_2 = 5.1 +/- 0.4 (mean +/- SEM, n = 4), (**Figure 3D** but not carbachol nor atropine, produced a similar increase in FRET.

Generation of VSV-G and SNAP-tagged hM_3 constructs

To further compare the functional properties of hM_3-R and hM_3-RASSL these forms of the receptor were tagged at the N-terminus with an anti-VSV-G epitope tag and the 20kDa SNAP-tag sequence (Alvarez-Curto et al., 2010). These forms were also expressed stably in Flp-In™ T-REx™ 293 cell lines. Following induction with doxycycline, addition of the cell impermeant, SNAP-tag specific substrate SNAP-488 allowed visual detection of cell surface-delivered forms of the receptors in intact cells (**Figure 4B**) because this substrate can link covalently to proteins that incorporate the SNAP-tag (Alvarez-Curto et al., 2010, Gautier et al., 2008, Ward et al., 2011). Receptor expression was confirmed and quantified firstly by performing saturation specific [^{3}H]QNB binding studies on membranes from cells treated with or without doxycycline. In cells induced to express VSV-G-SNAP hM_3-R [^{3}H]QNB bound with high affinity (K_D = 35 +/- 9 pM; mean +/- SEM) (**Figure 4C**). By contrast, in the

Molecular Pharmacology Fast Forward. Published on August 31, 2011 as DOI: 10.1124/mol.111.074674
This article has not been copyedited and formatted. The final version may differ from this version.

absence of doxycycline little specific [^{3}H]QNB binding was detected (not shown). As noted previously (Alvarez-Curto et al., 2010), following induction of expression of VSV-G-SNAP hM_3-RASSL, [^{3}H]QNB bound with appreciably lower affinity (K_D = 1.4 +/- 0.04 nM; mean +/- SEM)(**Figure 4D**). Atropine also displayed lower affinity at this RASSL variant than at the equivalent hM_3-R construct. Correction for receptor occupancy of measured IC_{50} values produced affinity estimates for atropine of 0.74 +/- 0.2 nM (mean +/- SEM, n = 3) for VSV-G-SNAP hM_3-R and 23 +/-1.4 nM (mean +/- SEM, n = 3) for VSV-G-SNAP hM_3-RASSL. Because of the need to use high concentrations of [^{3}H]QNB to approach a binding saturation isotherm for VSV-G-SNAP hM_3-RASSL this resulted in relatively poor specific to total binding values for [^{3}H]QNB. Expression of the two forms of the hM_3 receptor at the surface of cells was, therefore, further assessed via the binding to intact cells and associated luminescence intensity at 620 nm of a single concentration (20 nM) of SNAP-lumi4Tb. This is also able to bind covalently to the SNAP-tag present in the extracellular N-terminal domain of the constructs (Alvarez-Curto et al., 2010, Ward et al., 2011). Given the location of the SNAP-tag, this should be insensitive to the alterations in the [^{3}H]QNB binding pocket used to produce the hM_3-RASSL (**Figure 4E**). Virtually no binding of SNAP-lumi4Tb to either set of cells was noted in the absence of doxycycline but this increased over a range 1-10 ng.ml^{-1} of the antibiotic as expression of the corresponding receptor was induced, and was similar in the two cell lines (**Figure 4E**).

Analysis of ERK1/2 responses of the hM_3-R and hM_3-RASSL

There is currently great interest in the concept that different agonist ligands may selectively stabilize distinct conformations of a GPCR and thus potentially produce distinct signals or different patterns of regulation. This is generally referred to as 'functional selectivity' or 'ligand bias' (Smith et al., 2011, Mailman, 2007, Vaidehi and Kenakin, 2010, Kenakin, 2011, Violin and Lefkowitz, 2007). The

Molecular Pharmacology Fast Forward. Published on August 31, 2011 as DOI: 10.1124/mol.111.074674
This article has not been copyedited and formatted. The final version may differ from this version.

evolution of distinct molecular pairs of designer ligands and receptors makes assessment of the detailed function of such pairings of key importance before they can be employed widely, because there is no *a priori* reason to believe that they should function in an equivalent manner. We compared, therefore, effects of the endogenous agonist acetylcholine and its stable analog carbachol at the hM_3-R construct with those of clozapine N-oxide at the hM_3-RASSL. Cells induced to express VSV-G-SNAP hM_3-R or VSV-G-SNAP hM_3-RASSL by treatment with 5 $ng.ml^{-1}$ doxycycline were challenged with varying concentrations of acetylcholine, carbachol or clozapine N-oxide for 5 min and phospho-ERK1/2 levels subsequently measured. In cells induced to express VSV-G-SNAP hM_3-R both acetylcholine and carbachol produced robust, concentration-dependent increases (**Figure 5A, Table 1**) with acetylcholine being approximately 10 fold more potent than carbachol, pEC_{50}= 7.9 +/- 0.3 (n = 2) and pEC_{50} = 6.9 +/- 0.1 (n = 3), respectively. By contrast, even at 100 μM clozapine N-oxide was without effect (**Figure 5A**). The reverse was observed in cells induced to express VSV-G-SNAP hM_3-RASSL. Little or no response to carbachol or acetylcholine was observed at concentrations up to 100 μM whilst clozapine N-oxide produced a robust, concentration-dependent, increase in phospho-ERK1/2 with pEC_{50} = 7.6 +/- 0.4 (mean +/- SEM; n = 3) (**Figure 5B, Table 1**). Importantly, clozapine N-oxide did not appear to bind VSV-G-SNAP hM_3-R with significant affinity and potentially act as an antagonist because even in the presence of 100 μM clozapine N-oxide the concentration-response curve to carbachol was little affected (**Figure 5C**). Similarly 100 μM carbachol was unable to alter the concentration-response curve to clozapine N-oxide at VSV-G-SNAP hM_3-RASSL (**Figure 5D**). Subsequently, we assessed the kinetics of ERK1/2 phosphorylation in response to ligands in these cells. In cells induced to express VSV-G-SNAP hM_3-R both carbachol and acetylcholine promoted rapid and high level generation of

Molecular Pharmacology Fast Forward. Published on August 31, 2011 as DOI: 10.1124/mol.111.074674
This article has not been copyedited and formatted. The final version may differ from this version.

phospho-ERK1/2 (**Figure 6A**) and this was sustained over the course of at least 60 min (**Figure 6A**). By contrast, fetal bovine serum (20% (v/v)) used as a positive control, did not result in sustained ERK1/2 phosphorylation, although it did produce a peak of phospho-ERK1/2 within 5 min that rapidly decayed back to basal levels (**Figure 6A**). Neither atropine nor clozapine N-oxide promoted ERK1/2 phosphorylation at any time point measured. In VSV-G-SNAP hM_3-RASSL expressing cells treatment with clozapine N-oxide also resulted in sustained activation of ERK1/2 (**Figure 6B**) whilst, again, FBS produced a more modest response that was transient in nature (**Figure 6B**). In these cells both carbachol and acetylcholine (at 100 μM) did also cause a modest increase in ERK1/2 phosphorylation but in both theses cases the signal was as transitory as observed for FBS (**Figure 6B**).

Analysis of receptor internalization and interaction with β-arrestin-2

We next quantified the extent of receptor internalization in response to ligand challenge for 40 min by monitoring changes in FRET between the lumi4-Tb labelled receptor and Tag-lite® internalization buffer. VSV-G-SNAP-tagged hM_3-R and hM_3-RASSL expressing cells were labelled with 100 nM of the luminescent probe SNAP-lumi4-Tb and subsequently incubated with a mixture of Tag-lite® internalization reagent and receptor ligands (**Figure 7A, 7B**). At zero time, cell surface expression of each variant was detected. Internalization of the receptor variants following treatment of the cells with ligands was concentration-dependent with pEC_{50} = 4.8 +/- 0.16 (mean +/- SEM) for carbachol at the hM_3-R (**Figure 7A, Table 1**) and pEC_{50} = 6.2 +/- 0.15 (mean +/- SEM) for clozapine N-oxide at the hM_3-RASSL (**Figure 7A, Table 1**). In contrast, and as expected, the antagonist atropine (10 μM) did not elicit any detectable internalization of either receptor construct (not shown). As receptor

Molecular Pharmacology Fast Forward. Published on August 31, 2011 as DOI: 10.1124/mol.111.074674
This article has not been copyedited and formatted. The final version may differ from this version.

internalization is often preceded by interactions with a β-arrestin we also assessed the potential interaction of both hM_3-R and hM_3-RASSL forms with β-arrestin-2. HEK293T cells were transiently co-transfected with β-arrestin -2-*Renilla* luciferase 8 and either Flag-hM_3-R-Citrine (Alvarez-Curto et al., 2010) or a similar construct containing the RASSL variant but with an N-terminal c-Myc tag. Addition of colenterazine-h to such cells resulted in bioluminescence resonance energy transfer (BRET) that was produced in a concentration-dependent manner by both acetylcholine and carbachol in cells expressing Flag-hM_3-R-Citrine, and with similar potencies (carbachol pEC_{50} = 4.4 +/- 0.5; n = 4; acetylcholine pEC_{50} = 4.6 +/- 0.4; n = 4) (**Figure 7C**). No such effect was produced by clozapine N-oxide (**Figure 7C**). By contrast, in cells expressing c-Myc-hM_3-RASSL-Citrine, clozapine N-oxide potently enhanced BRET signals (pEC_{50} = 6.4 +/- 0.3, n=3) whilst acetylcholine and carbachol produced no significant effects at concentrations up to 1 mM (**Figure 7D**).

Analysis of the phosphorylation status of hM_3-R and hM_3-RASSL

We have previously demonstrated that the M_3-receptor is phosphorylated on multiple sites in response to agonist occupation (Butcher et al., 2011). We have also presented evidence that the nature of receptor phosphorylation is influenced not only by the cell type in which the receptor is expressed but also by the ligand used to stimulate the receptor (Butcher et al., 2011). We have proposed that the difference in the profile of receptor phosphorylation seen within different cell types might represent a phosphorylation bar-code that can direct signalling (Tobin et al, 2008, Tobin, 2008). In light of these observations we assessed whether or not clozapine N-oxide could induce phosphorylation of the hM_3-RASSL and, if so, whether the profile of receptor phosphorylation, and thereby the phosphorylation bar-code, was comparable to that observed for hM_3-R stimulated by acetylcholine.

Molecular Pharmacology Fast Forward. Published on August 31, 2011 as DOI: 10.1124/mol.111.074674
This article has not been copyedited and formatted. The final version may differ from this version.

Metabolic labelling of Flp-In™ T-REx™ 293 cells expressing VSV-G-SNAP hM_3-R or VSV-G-SNAP hM_3-RASSL with [^{32}P]-orthophosphate followed by immunoprecipitation of the receptors using a receptor-specific antibody was used to determine the receptor-phosphorylation status (**Figure 8**). Using this approach it was determined that both hM_3-R and hM_3-RASSL receptors were phosphorylated in the basal state (**Figure 8B**). In these experiments the receptor appeared as a band running at 125kDa in SDS-PAGE that was present only in cells induced with doxycycline to express the receptor (**Figure 8A, B**). Consistent with the ligand binding and functional data presented above, hM_3-R showed increased phosphorylation in response to acetylcholine but showed no change in phosphorylation upon addition of clozapine N-oxide. In contrast, phosphorylation of VSV-G-SNAP hM_3-RASSL was increased only by clozapine N-oxide (**Figure 8B**). To examine the pattern of phosphorylation the immunoprecipitated receptors were partially digested with trypsin before 2-dimensional resolution. This approach has been used previously to determine the pattern of muscarinic receptor phosphorylation (Butcher et al., 2011, Torrecilla et al., 2007). Here the pattern of phosphorylation of hM_3-R in response to acetylcholine was very similar to the pattern of phosphorylation observed for the hM_3-RASSL in response to clozapine N-oxide (**Figure 8C**).

We further probed individual sites of phosphorylation with phospho-specific antibodies that react with pS412 within the IL3, or pS577 within the C-terminal tail (Butcher et al., 2011). Acetylcholine acting at hM_3-R and clozapine N-oxide acting at hM_3-RASSL increased to a similar extent the phosphorylation of sites pS412 (**Figure 9A**) and pS577 (**Figure 9B**). These studies indicated that the phosphorylation status of the hM_3-RASSL in response to clozapine N-oxide was very similar to that observed for the hM_3-R in response to the endogenous ligand acetylcholine.

Molecular Pharmacology Fast Forward. Published on August 31, 2011 as DOI: 10.1124/mol.111.074674
This article has not been copyedited and formatted. The final version may differ from this version.

The basis for ligand selectivity of the RASSL

Although the results of the chemical genetic engineering are clear cut, the molecular basis for this is less obvious. In the case of loss of potency and/or affinity for acetylcholine and carbachol (and muscarinic antagonists), the importance of D3.32 in providing a charge partner for the positively charged ligand is well established. Y3.33, located next to D3.32, is also postulated to make a cation-pi interaction with acetylcholine and, together with D3.32, to keeps the charge fixed in space (Grauert et al., 2010). To attempt to understand why these alterations also result in enhanced potency and/or affinity for clozapine N-oxide, homology models (Grauert et al., 2010, Tautermann, 2011) of the hM_3-R were generated and used initially to predict the mode of binding of clozapine, which is known to have modest affinity for hM_3-R. Here the charged center of the piperazine moiety interacts with D3.32 allowing the rest of the molecule to fit within the orthosteric binding site. However, in hM_3-R, Y3.33 clashes with the ligand and its replacement by cysteine in the hM_3-RASSL makes the interaction of ligand and receptor easier (**Figure 10**). Furthermore, in hM_3-R tyrosines at positions 6.51 and 7.39, along with Y3.33, form a roof to the aromatic pocket where the charged part of M_3 ligands bind. In the RASSL one side of this is absent and, hence, ligands may move slightly. This was observed when docking clozapine, in which the NH-group from the dibenzo[1,4]diazepine core interacts with T5.42, a residue required for activation of the M_3-R by acetylcholine (Wess et al., 1992). The A5.46G mutation makes further space for clozapine to interact with T5.42. It is important to note for validation of the model, therefore, that clozapine has been reported to be 100 fold more potent in Ca^{2+} assays at the hM_3-RASSL than at hM_3-R (Armbruster et al., 2007). Interestingly, clozapine N-oxide does not fit well into the binding site of hM_3-R because it lacks the positively charged head-group to interact with D3.32, explaining its lack of potency/affinity at the wild type and

Molecular Pharmacology Fast Forward. Published on August 31, 2011 as DOI: 10.1124/mol.111.074674
This article has not been copyedited and formatted. The final version may differ from this version.

the inability to compete with carbachol/acetylcholine as shown in Figure 5. However, on the basis that it would be likely to dock into hM_3-R in a similar orientation as clozapine, interactions in the aromatic/D3.32 cage are poor with the piperazine-N-oxide group, therefore the ligand moves slightly away from D3.32, causing the opening of the roof of the binding pocket (i.e., the network of tyrosines 3.33 and 6.51, 7.39 is interrupted) and upward movement (**Figure 10**). Thus, even if clozapine N-oxide is able to bind with low affinity to hM_3-R (and the data of Figure 5 indicate any such affinity to be very low) no interaction can be formed with T5.42, thus no agonist action would be expected. In contrast, for hM_3-RASSL, the roof of the aromatic cage binding site does not exist and clozapine N-oxide thus does not need to break this energetically favorable interaction. The piperazine-N-oxide interacts with the aromatic cage (the N is closer to D3.32 and the O is close to C7.42 – possibly allowing a hydrogen bond interaction) and the aromatic part of the molecule moves towards transmembrane domain 5, interacting with T5.42 (**Figure 10**). Also here the mutation A5.46G allows clozapine N-oxide to come closer to and interact with T5.42. As noted previously (Alvarez-Curto et al., 2010), the affinity of hM_3-RASSL constructs to bind muscarinic antagonists, including [^{3}H]QNB and atropine, was significantly lower than the hM_3-R forms. This was not unexpected as these ligands interact with many of the same residues as acetylcholine and are competitive with the endogenous ligand.

DISCUSSION

Our study is the first to comprehensively test if synthetic ligands acting at a RASSL receptor are able to mediate receptor responses that are similar to those of the natural ligand operating at the wild type receptor. Such analysis is critical in validation of the use of RASSL receptors in transgenic studies designed to test the function of GPCRs and in the use of such RASSLs in defining selective GPCRs as

Molecular Pharmacology Fast Forward. Published on August 31, 2011 as DOI: 10.1124/mol.111.074674
This article has not been copyedited and formatted. The final version may differ from this version.

therapeutic targets. Recent studies that have determined that different GPCR ligands can stabilize or induce different conformations of a receptor and that these can differentially engage G protein subtypes and other downstream signalling proteins in a process called functional selectivity or ligand bias, raises the very real possibility that synthetic ligands acting on RASSL receptors might show bias that will result in a different signalling profile of the RASSL receptor from the wild type. Given this possibility and the huge experimental potential of RASSL receptors it would seem essential that careful characterization of the signalling properties of such receptor mutants must be addressed.

We approach this question here by using a RASSL of the hM_3-muscarinic receptor that was developed on the basis that the drug clozapine has relatively low affinity/potency at muscarinic receptor subtypes and the related molecule clopazine N-oxide is essentially inactive. Armbruster and colleagues hence scanned randomly generated point mutants of the M_3-receptor for loss of potency to acetylcholine and a concurrent gain of potency to clopazine N-oxide (Armbruster et al., 2007). They noted that by combining two point mutants in the M_3 receptor, cysteine for tyrosine at position 3.33 and glycine for alanine at position 5.46 (Armbruster et al., 2007), a large alteration in the potency ratio in favour of clozapine N-oxide over acetylcholine was achieved. Moreover, as the amino acids at positions 3.33 and 5.46 are conserved in the other 4 muscarinic receptor subtypes the same alterations result in similar changes in pharmacology (Armbruster et al., 2007). In the various approaches used herein it would be anticipated that the potency of ligands in the intramolecular FRET studies and in both the internalization and β-arrestin-2 interaction studies should provide reasonable surrogate estimates of agonist affinity as each of these is linked closely to receptor occupancy. By contrast, signals measured downstream, i.e. elevation of intracellular Ca^{2+} and ERK1/2 MAP kinase phosphorylation, involve

Molecular Pharmacology Fast Forward. Published on August 31, 2011 as DOI: 10.1124/mol.111.074674
This article has not been copyedited and formatted. The final version may differ from this version.

amplification and therefore the presence of receptor reserve accounts for the lower concentrations of ligands required to produce half-maximal effects. Indeed, the results from the assays linked closely to receptor occupancy indicate that acetylcholine has affinity estimated in the region of 10 μM for the various forms of hM_3-R used whilst clozapine N-oxide has affinity estimated as close to 1 μM for the hM_3-RASSL forms (**Table 1**).

Functionality of agonist ligands can be assessed at many levels within signal transduction cascades and to define the equivalence (or otherwise) of action of acetylcholine at hM_3-R and clozapine N-oxide at the hM_3-RASSL variants we employed a wide range of assays. Initial conformational changes of receptors upon binding of an agonist can be monitored by intramolecular FRET studies if appropriate FRET donor and acceptor species are integrated into sites within the receptor that move or re-orientate relative to one another upon agonist binding. As observations from agonist-bound atomic level structures of GPCRs (Xu et al, 2011, Rosenbaum et al., 2011) have supported earlier predictions about outward movement of the intracellular end of transmembrane domain 6, then alterations in FRET signal within a receptor are anticipated if a FRET acceptor in placed in the third intracellular loop, as this links transmembrane domains 5 and 6, and a FRET donor is linked to the C-terminal tail of the receptor (Hoffmann et al., 2005, Zurn et al., 2009). Such an intramolecular FRET sensor has been validated previously for the hM_3-R (Ziegler et al., 2011). In initial studies we introduced both Y3.33C and A5.46G mutations to produce the hM_3-RASSL and also assessed the effect on response to both clozapine N-oxide and acetylcholine/carbachol on equivalent sensors expressing either mutation in isolation. As these studies validated the anticipated responsiveness of the sensors we generated stably transfected cell lines able to express either the hM_3-R or hM_3-RASSL sensor and used them to generate concentration response data.

Molecular Pharmacology Fast Forward. Published on August 31, 2011 as DOI: 10.1124/mol.111.074674
This article has not been copyedited and formatted. The final version may differ from this version.

Although some aspects of signal generation of the hM_3-RASSL and comparisons with the wild type receptor have been assessed previously (Armbruster et al., 2007) as a prelude to generation of transgenic animals expressing this variant, these were very limited in scope and were performed prior to recent studies that have determined that subtle variation in receptor conformation (mediated by receptor mutations or the binding of different ligands) can have a profound impact on the signalling outcomes of a receptor. Nor did these earlier studies fully appreciate our developing understanding of biased signalling and functional selectivity – all of which are potential mechanisms by which RASSL receptors might mediate distinct signal profiles from that of wild type receptors. This means that, in retrospect, the initial studies (Armbruster et al., 2007) were too superficial to conclude that such RASSL receptors signal in a manner equivalent to the wild type receptors.

We have previously used cell lines able to express versions of the hM_3-R and hM_3-RASSL, modified to incorporate SNAP-tags in their extracellular N-terminal domain, to employ time-resolved FRET studies based on Tag-lite® reagents to explore the quaternary organization of cell surface hM_3 receptors (Alvarez-Curto et al, 2010). Internalization of each form of hM_3 was produced only in response to the anticipated ligands and, at maximally effective ligand concentration, was of similar extent. Equally, hM_3-R and hM_3-RASSL variants were able to interact with β-arrestin-2 only in response to the appropriate agonists and in a ligand concentration-dependent manner. Integrated measures of downstream signal transduction were also compared by assessing phosphorylation of the ERK1/2 MAP kinases. In both cases this effect was extensive and was maintained for a prolonged period. There was no indication of differences in levels of constitutive activity between the hM_3-R and hM_3-RASSL as ERK1/2 phosphorylation in the absence of agonist ligands was not different. In contrast to activation of the forms of hM_3, ERK1/2 phosphorylation

promoted by FBS in each cell line was transitory in nature, returning to basal levels within a 15 min period. Transient ERK1/2 phosphorylation was also noted to both acetylcholine and carbachol in cells expressing hM_3-RASSL. Although we have not explored this in detail, it is likely to reflect the known endogenous expression of low levels of hM_3-R in HEK293 derived cells (Shaw et al., 2002) whilst activation of the endogenous receptor in cells expressing the hM_3-R sensor are presumably masked by the large response generated by the sensor.

A key assessment of the likely equivalence of activation of hM_3-R by acetylcholine and hM_3-RASSL by clozapine N-oxide was performed in studies that assessed the extent of phosphorylation of the receptor variants following addition of agonists. Analysis of either the global pattern of phosphorylation using tryptic phospho-peptide maps or analysis of individual sites of phosphorylation using receptor phospho-specific antibodies showed there to be no significance difference in the phosphorylation profile of the wild type hM_3-R and the hM_3-RASSL mutant.

This is important in light of recent studies that have indicated that the pattern of receptor phosphorylation can contribute to the signalling outcome of the receptor (Poulin et al., 2010 Tobin et al., 2008). Thus, if the phosphorylation pattern, or phosphorylation bar-code, between the hM_3-RASSL and hM_3-R were different then this might suggest that the signalling of the two receptors might be different. The fact that the phosphorylation pattern was equivalent between the receptor variants following agonist stimulation would point to the likelihood that the signalling outcomes of these receptors would be equivalent. This conclusion is consistent with the fact that we show here that ERK-1/2 activation, β-arrestin recruitment and receptor internalization of the hM_3-RASSL and hM_3-R following stimulation with clozapine-N-oxide and acetylcholine, respectively, was similar.

Molecular Pharmacology Fast Forward. Published on August 31, 2011 as DOI: 10.1124/mol.111.074674
This article has not been copyedited and formatted. The final version may differ from this version.

Our studies, therefore, indicate that the response of the hM_3-RASSL to clozapine-N-oxide is very similar to that of the hM_3-R to acetylcholine. This is important since analysis of the binding characteristics of clozapine-N-oxide carried out here indicates that the mechanism of receptor activation of the hM_3-RASSL is subtly different from that of acetylcholine activation of hM_3-R. Given that there is now accumulating evidence that different orthosteric ligands to GPCRs can drive different signalling outcomes in a process called ligand bias or functional selectively (Smith et al., 2011, Mailman, 2007, Kenakin, 2011), there is a possibility that the subtle differences in the activation mechanism of the hM_3-RASSL and hM_3-R might manifest itself in differences in the signalling properties of these receptor variants. The detailed analysis carried out here indicates that there is no functional selectivity associated with clozapine-N-oxide at the hM_3-RASSL. This validates the use of this particular RASSL receptor mutant in transgenic studies of receptor action where the pharmacological stimulation of the hM_3-RASSL expressed in a genetically engineered mouse strain is presumed to mimic the actions of the wild type hM_3-R. In light of our study we can view with confidence data generated from the used the hM_3-RASSL receptor in neuronal (Alexander et al., 2009) and pancreatic studies (Guettier et al., 2009) and pursue future transgenic studies in our own laboratory aimed at conditionally expressing the hM_3-RASSL in place of the wild type hM_3-R.

Despite these results the ongoing production of novel RASSLs from different parental receptors cautions that equivalent studies to these must be performed routinely as a prelude to their *in vivo* expression and analysis of function.

AUTHORSHIP CONTRIBUTIONS

Participated in research design: Alvarez-Curto, Tobin, Milligan

Conducted experiments: Alvarez-Curto, Prihandoko, Pediani, Tautermann

Contributed new reagents or analytical tools: Hoffmann, Lohse, Zwier, Tobin

Molecular Pharmacology Fast Forward. Published on August 31, 2011 as DOI: 10.1124/mol.111.074674
This article has not been copyedited and formatted. The final version may differ from this version.

Performed data analysis: Alvarez-Curto, Pediani, Prihandoko, Tautermann, Tobin, Milligan

Wrote or contributed to the writing of the manuscript: Milligan, Tobin, Alvarez-Curto with contributions from all authors

Other:

Molecular Pharmacology Fast Forward. Published on August 31, 2011 as DOI: 10.1124/mol.111.074674
This article has not been copyedited and formatted. The final version may differ from this version.

REFERENCES

Alexander GM, Rogan SC, Abbas AI, Armbruster BN, Pei Y, Allen JA, Nonneman RJ, Hartmann J, Moy SS, Nicolelis MA, McNamara JO and Roth BL (2009) Remote control of neuronal activity in transgenic mice expressing evolved G protein-coupled receptors. *Neuron* **63**(1):27-39.

Alvarez-Curto E, Ward RJ, Pediani JD and Milligan G (2010) Ligand regulation of the quaternary organization of cell surface M3 muscarinic acetylcholine receptors analyzed by fluorescence resonance energy transfer (FRET) imaging and homogeneous time-resolved FRET. *J Biol Chem* **285**(30):23318-23330.

Armbruster BN, Li X, Pausch MH, Herlitze S and Roth BL (2007) Evolving the lock to fit the key to create a family of G protein-coupled receptors potently activated by an inert ligand. *Proc Natl Acad Sci U S A* **104**(12):5163-5168.

Ballesteros JA and Weinstein H (1995) Integrated methods for the construction of three dimensional models and computational probing of structure-function relations in G-protein coupled receptors. *Methods Neurosci* **25**:*366-428*.

Bhattacharya S, Hall SE, Li H and Vaidehi N (2008) Ligand-stabilized conformational states of human beta(2) adrenergic receptor: insight into G-protein-coupled receptor activation. *Biophys J* **94**(6):2027-2042.

Butcher AJ, Prihandoko R, Kong KC, McWilliams P, Edwards JM, Bottrill A, Mistry S and Tobin AB (2011) Differential G-protein-coupled receptor phosphorylation provides evidence for a signaling bar code. *J Biol Chem* **286**(13):11506-11518.

Chang WC, Ng JK, Nguyen T, Pellissier L, Claeysen S, Hsiao EC and Conklin BR (2007) Modifying ligand-induced and constitutive signaling of the human 5-HT4 receptor. *PLoS One* **2**(12):e1317.

Conklin BR, Hsiao EC, Claeysen S, Dumuis A, Srinivasan S, Forsayeth JR, Guettier JM, Chang WC, Pei Y, McCarthy KD, Nissenson RA, Wess J, Bockaert J and Roth BL (2008) Engineering GPCR signaling pathways with RASSLs. *Nat Methods* **5**(8):673-678.

Conn PJ, Jones CK and Lindsley CW (2009) Subtype-selective allosteric modulators of muscarinic receptors for the treatment of CNS disorders. *Trends Pharmacol Sci* **30**(3):148-155.

Digby GJ, Shirey JK and Conn PJ (2010) Allosteric activators of muscarinic receptors as novel approaches for treatment of CNS disorders. *Mol Biosyst* **6**(8):1345-1354.

Dong S, Rogan SC and Roth BL (2010) Directed molecular evolution of DREADDs: a generic approach to creating next-generation RASSLs. Nat Protoc 5(3):561-573.

Ellis J, Pediani JD, Canals M, Milasta S and Milligan G (2006) Orexin-1 receptor-cannabinoid CB1 receptor heterodimerization results in both ligand-dependent and -independent coordinated alterations of receptor localization and function. J Biol Chem 281(50):38812-38824.

Gautier A, Juillerat A, Heinis C, Corrêa IR Jr, Kindermann M, Beaufils F, Johnsson K. (2008) An engineered protein tag for multiprotein labeling in living cells. Chem Biol. 15 (2):128-36

Guettier JM, Gautam D, Scarselli M, Ruiz de Azua I, Li JH, Rosemond E, Ma X, Gonzalez FJ, Armbruster BN, Lu H, Roth BL and Wess J (2009) A chemical-genetic approach to study G protein regulation of beta cell function in vivo. *Proc Natl Acad Sci U S A* **106**(45):19197-19202.

Hoffmann C, Gaietta G, Bunemann M, Adams SR, Oberdorff-Maass S, Behr B, Vilardaga JP, Tsien RY, Ellisman MH and Lohse MJ (2005) A FlAsH-based

FRET approach to determine G protein-coupled receptor activation in living cells. *Nat Methods* **2**(3):171-176.

Jenkins L, Alvarez-Curto E, Campbell K, de Munnik S, Canals M, Schlyer S and Milligan G (2011) Agonist activation of the G protein-coupled receptor GPR35 involves transmembrane domain III and is transduced via Galpha and beta-arrestin-2. *Br J Pharmacol* **162**(3):733-748.

Jenkins L, Brea J, Smith NJ, Hudson BD, Reilly G, Bryant NJ, Castro M, Loza MI and Milligan G (2010) Identification of novel species-selective agonists of the G-protein-coupled receptor GPR35 that promote recruitment of beta-arrestin-2 and activate Galpha13. *Biochem J* **432**(3):451-459.

Kenakin T (2011) Functional selectivity and biased receptor signaling. *J Pharmacol Exp Ther* **336**(2):296-302.

Kobilka BK and Deupi X (2007) Conformational complexity of G-protein-coupled receptors. *Trends Pharmacol Sci* **28**(8):397-406.

Mailman RB (2007) GPCR functional selectivity has therapeutic impact. *Trends Pharmacol Sci* **28**(8):390-396.

Nawaratne V, Leach K, Suratman N, Loiacono RE, Felder CC, Armbruster BN, Roth BL, Sexton PM and Christopoulos A (2008) New insights into the function of M4 muscarinic acetylcholine receptors gained using a novel allosteric modulator and a DREADD (designer receptor exclusively activated by a designer drug). *Mol Pharmacol* **74**(4):1119-1131.

Pei Y, Rogan SC, Yan F and Roth BL (2008) Engineered GPCRs as tools to modulate signal transduction. *Physiology (Bethesda)* **23**:313-321.

Poulin B, Butcher A, McWilliams P, Bourgognon JM, Pawlak R, Kong KC, Bottrill A, Mistry S, Wess J, Rosethorne EM, Charlton SJ and Tobin AB (2010) The M3-muscarinic receptor regulates learning and memory in a receptor

phosphorylation/arrestin-dependent manner. *Proc Natl Acad Sci U S A* **107**(20):9440-9445.

Rajagopal S, Rajagopal K and Lefkowitz RJ (2010) Teaching old receptors new tricks: biasing seven-transmembrane receptors. *Nat Rev Drug Discov* **9**(5):373-386.

Redfern CH, Coward P, Degtyarev MY, Lee EK, Kwa AT, Hennighausen L, Bujard H, Fishman GI and Conklin BR (1999) Conditional expression and signaling of a specifically designed Gi-coupled receptor in transgenic mice. *Nat Biotechnol* **17**(2):165-169.

Rosenbaum DM, Zhang C, Lyons JA, Holl R, Aragao D, Arlow DH, Rasmussen SG, Choi HJ, Devree BT, Sunahara RK, Chae PS, Gellman SH, Dror RO, Shaw DE, Weis WI, Caffrey M, Gmeiner P and Kobilka BK (2011) Structure and function of an irreversible agonist-beta(2) adrenoceptor complex. *Nature* **469**(7329):236-240.

Shaw G, Morse S, Ararat M and Graham FL (2002) Preferential transformation of human neuronal cells by human adenoviruses and the origin of HEK 293 cells. *FASEB J* **16**(8):869-871.

Smith NJ, Bennett KA and Milligan G (2011) When simple agonism is not enough: emerging modalities of GPCR ligands. *Mol Cell Endocrinol* **331**(2):241-247.

Smith NJ, Stoddart LA, Devine NM, Jenkins L and Milligan G (2009) The action and mode of binding of thiazolidinedione ligands at free fatty acid receptor 1. *J Biol Chem* **284**(26):17527-17539.

Stoddart LA, Smith NJ, Jenkins L, Brown AJ and Milligan G (2008) Conserved polar residues in transmembrane domains V, VI, and VII of free fatty acid receptor 2 and free fatty acid receptor 3 are required for the binding and function of short chain fatty acids. *J Biol Chem* **283**(47):32913-32924.

Swaminath G, Deupi X, Lee TW, Zhu W, Thian FS, Kobilka TS and Kobilka B (2005) Probing the beta2 adrenoceptor binding site with catechol reveals differences in binding and activation by agonists and partial agonists. *J Biol Chem* **280**(23):22165-22171.

Sweger EJ, Casper KB, Scearce-Levie K, Conklin BR and McCarthy KD (2007) Development of hydrocephalus in mice expressing the G(i)-coupled GPCR Ro1 RASSL receptor in astrocytes. *J Neurosci* **27**(9):2309-2317.

Tautermann CS (2011) The use of G-protein coupled receptor models in lead optimization. *Future Med Chem* **3**(6):709-721.

Tobin AB (2008) G-protein-coupled receptor phosphorylation: where, when and by whom. *Br J Pharmacol* **153 Suppl 1**:S167-176.

Tobin AB, Butcher AJ and Kong KC (2008) Location, location, location...site-specific GPCR phosphorylation offers a mechanism for cell-type-specific signalling. *Trends Pharmacol Sci* **29**(8):413-420.

Torrecilla I, Spragg EJ, Poulin B, McWilliams PJ, Mistry SC, Blaukat A and Tobin AB (2007) Phosphorylation and regulation of a G protein-coupled receptor by protein kinase CK2. *J Cell Biol* **177**(1):127-137.

Vaidehi N and Kenakin T (2010) The role of conformational ensembles of seven transmembrane receptors in functional selectivity. *Curr Opin Pharmacol* **10**(6):775-781.

Verkaar F, van Rosmalen JW, Blomenrohr M, van Koppen CJ, Blankesteijn WM, Smits JF and Zaman GJ (2008) G protein-independent cell-based assays for drug discovery on seven-transmembrane receptors. *Biotechnol Annu Rev* **14**:253-274.

Violin JD and Lefkowitz RJ (2007) Beta-arrestin-biased ligands at seven-transmembrane receptors. *Trends Pharmacol Sci* **28**(8):416-422.

Ward RJ, Pediani JD and Milligan G (2011) Ligand-induced internalization of the orexin OX(1) and cannabinoid CB(1) receptors assessed via N-terminal SNAP and CLIP-tagging. *Br J Pharmacol* **162**(6):1439-1452.

Wess J (2004) Muscarinic acetylcholine receptor knockout mice: novel phenotypes and clinical implications. *Annu Rev Pharmacol Toxicol* **44**:423-450.

Wess J, Eglen RM and Gautam D (2007) Muscarinic acetylcholine receptors: mutant mice provide new insights for drug development. *Nat Rev Drug Discov* **6**(9):721-733.

Wess J, Maggio R, Palmer JR and Vogel Z (1992) Role of conserved threonine and tyrosine residues in acetylcholine binding and muscarinic receptor activation. A study with m3 muscarinic receptor point mutants. *J Biol Chem* **267**(27):19313-19319.

Xu F, Wu H, Katritch V, Han GW, Jacobson KA, Gao ZG, Cherezov V and Stevens RC (2011) Structure of an agonist-bound human A2A adenosine receptor. *Science* **332**(6027):322-327.

Ziegler N, Batz J, Zabel U, Lohse MJ and Hoffmann C (2011) FRET-based sensors for the human M1-, M3-, and M5-acetylcholine receptors. *Bioorg Med Chem* **19**(3):1048-1054.

Zurn A, Zabel U, Vilardaga JP, Schindelin H, Lohse MJ and Hoffmann C (2009) Fluorescence resonance energy transfer analysis of alpha 2a-adrenergic receptor activation reveals distinct agonist-specific conformational changes. *Mol Pharmacol* **75**(3):534-541.

Molecular Pharmacology Fast Forward. Published on August 31, 2011 as DOI: 10.1124/mol.111.074674
This article has not been copyedited and formatted. The final version may differ from this version.

FOOTNOTES

These studies were supported by grants from the Biotechnology and Biosciences Research Council [BB/E006302/1]; the Medical Research Council [G0900050]; the Wellcome Trust [047600]; and a Biotechnology and Biosciences Research Council - Heptares Inc studentship [RM36G0146].

Tag-lite(r) and lumi4(r) are registered trademarks of Cisbio Bioassays. Lumi4 is a registered trademark of Lumiphore, Inc.

Address for reprint requests: Graeme Milligan, Wolfson Link Building 253, University of Glasgow, Glasgow G12 8QQ, Scotland, U.K.. e-mail: Graeme.Milligan@glasgow.ac.uk or Andrew B. Tobin Department of Cell Physiology and Pharmacology, University of Leicester, Hodgkin Building, Lancaster Road, Leicester LE1 9HN, England, U.K. e-mail: tba@leicester.ac.uk

Molecular Pharmacology Fast Forward. Published on August 31, 2011 as DOI: 10.1124/mol.111.074674
This article has not been copyedited and formatted. The final version may differ from this version.

LEGENDS FOR FIGURES

Figure 1 Ligand regulation of intramolecular hM_3 FRET sensor variants: from hM_3-R to hM_3 -RASSL

HEK293T cells were transfected transiently to express following FlAsH-eCFP FRET sensors: hM_3 FlAsH (**A**), Y149C hM_3 FlAsH (**B**) A239G hM_3 FlAsH (**C**) or Y149C + A239G hM_3 FlAsH (RASSL) (**D**). These were exposed for 15 seconds (see bar) to 1 mM carbachol (red trace) or either 100 μM (blue trace) or 10 μM (light blue trace) (only in **D**) clozapine N-oxide. Traces represent mean +/- SEM from 10-15 cells individual cells.

Figure 2 Expression and function of intramolecular FRET sensor forms of the hM_3 receptor

Membranes were prepared from untreated cells (- dox) harboring hM_3-R (**A**) or hM_3 RASSL (**B**) intramolecular FRET sensors or those induced (+ dox) to express the constructs. These were used to measure the specific binding of varying concentration of [^{3}H]QNB. Two further experiments produced similar results. **C.** Calcium mobilization in response to varying concentrations of acetylcholine (Ach) and carbachol (Cch) at the hM_3-R and to clozapine N-oxide (CNO) and Cch at the hM_3-RASSL is shown. Data represent means +/_ SEM of triplicate assays from a single experiment. Two further experiments produced similar results.

Molecular Pharmacology Fast Forward. Published on August 31, 2011 as DOI: 10.1124/mol.111.074674
This article has not been copyedited and formatted. The final version may differ from this version.

Figure 3 Appropriate agonists selectively modulate intramolecular FRET sensor forms of the hM_3

MOL #74674

A. Cartoon of the hM_3-R intramolecular FRET sensors shows the relative positioning of the introduced FlAsH sequence and the appended eCFP. Circles represent the amino acids mutated to generate the RASSL variant. **B.** Cells induced to express the hM_3-R FRET sensor were labelled with lumiogreen and imaged (FlAsH) or imaged to detect eCFP (eCFP). Expression of the hM_3-R (**C**) or hM_3-RASSL (**D**) intramolecular FRET sensors was induced and concentration-response curves to carbachol at the hM_3-R (**C**) and CNO at the hM_3-RASSL (**D**) variants were constructed based on the maximal amplitude of the FRET sensor response. Data are mean +/- SEM from 10-15 cells individual cells.

Figure 4 Expression and detection of VSV-G- and SNAP-tagged forms of hM_3 receptor

VSV-G and SNAP-tag sequences were added at the N-terminus of either hM_3-R or hM_3-RASSL. A signal sequence derived from the metabotropic glutamate receptor 5 was also included at the extreme N-terminus as described previously (Alvarez-Curto et al., 2010). A cartoon representation of the constructs is illustrated (**A**) in which the circles represent amino acids mutated to generate the RASSL variant. Following the production of Flp-In^{TM} T-REx^{TM} 293 lines harboring either of these constructs at the inducible locus, cells maintained on glass cover slips were treated with doxycycline (5 ng.ml^{-1}, 24h) and following addition of SNAP-488 (5 µM, 30 min) these were imaged (**B**). Membranes prepared from cells induced to express VSV-G-SNAP hM_3-R (**C**) or VSV-G-SNAP hM_3-RASSL (**D**) were used to measure the specific binding of

Molecular Pharmacology Fast Forward. Published on August 31, 2011 as DOI: 10.1124/mol.111.074674
This article has not been copyedited and formatted. The final version may differ from this version.

varying concentrations of [^{3}H]QNB. Intact cells harboring VSV-G-SNAP hM$_3$-R (**light bars**) or VSV-G-SNAP hM$_3$-RASSL (**dark bars**) were untreated (no dox) or treated

with the indicated concentrations of doxycycline for 24 h. Subsequently 20nM SNAP-lumi4Tb was added for 1 h and after washing, luminescence intensity at 620 nm measured after excitation at 337nm (**E**). Data are means +/-SEM of triplicate assays from 2 independent experiments.

Figure 5 Selective activation of ERK1/2 phosphorylation via VSV-G-SNAP hM$_3$-R or VSV-G-SNAP hM$_3$-RASSL

Flp-In™ T-REx™ 293 cells harboring VSV-G-SNAP hM$_3$-R (**A, C**) or VSV-G-SNAP hM$_3$-RASSL (**B, D**) were induced to express these constructs by treatment with doxycycline (5 ng.ml^{-1}, 24h). Subsequently cells were stimulated for 5 min with varying concentrations of acetylcholine (Ach), carbachol (Cch) or clozapine N-oxide (CNO) and ERK1/2 phosphorylation assessed using the AlphaScreen® Surefire® kit. In **C**, the effect of varying concentrations of carbachol was assessed in the concurrent presence of 100 μM clozapine N-oxide whilst in **D** the effect of varying concentrations of clozapine N-oxide was assessed in the presence of 100 μM carbachol. Data represent means +/- SEM from 3 experiments.

Figure 6 Equivalent and sustained kinetics of ERK1/2 phosphorylation via VSV-G-SNAP hM$_3$-R or VSV-G-SNAP hM$_3$-RASSL

The ability of carbachol (Cch), acetylcholine (Ach) and clozapine N-oxide (CNO) to stimulate ERK1/2 phosphorylation was assessed at various times of exposure to ligands (all 100 μM) in cells induced to express VSV-G-SNAP hM$_3$-R (**A**) or VSV-G-SNAP hM$_3$-RASSL (**B**) as in Figure 5. The lack of effect of atropine and a transient

Molecular Pharmacology Fast Forward. Published on August 31, 2011 as DOI: 10.1124/mol.111.074674
This article has not been copyedited and formatted. The final version may differ from this version.

effect of fetal bovine serum (FBS) were also recorded in both cell lines. Data represent means +/- SEM from 4 experiments

Figure 7 Appropriate agonists promote internalization of variants of the hM_3 receptor and interactions of the receptors with β-arrestin-2

VSV-G-and SNAP-tagged hM_3-R and hM_3-RASSL expressing cells were labelled with 100 nM of the luminescent probe SNAP-Lumi4-Tb and subsequently incubated with a mixture of Tag-lite® internalization reagent and carbachol (Cch), clozapine N-oxide (CNO) for 0 or 40 min (**A, B**). HEK293T cells were transiently co-transfected with β-arrestin-2-*Renilla* luciferase 8 and either Flag-hM_3-Citrine (**C**) or c-Myc-hM_3-RASSL-Citrine (**D**). Following addition of varying concentrations of acetylcholine (Ach), carbachol (Cch) or clozapine N-oxide (CNO) for 10 min, colenterazine-h was added and BRET measured as a surrogate for the recruitment of β-arrestin-2 to the forms of the hM_3 receptor. (Data are means +/_ SEM from either 3 or 4 independent experiments performed in triplicate.

Figure 8 Appropriate agonists regulate similar patterns of phosphorylation on the hM_3 receptor variants

Flp-In™ T-REx™ 293 cells harboring VSV-G-SNAP hM_3-R (**A, left**) or VSV-G-SNAP hM_3-RASSL (**A, right**) were uninduced (no dox) or induced to express these constructs by treatment with doxycycline (2 $ng.ml^{-1}$, 24h). Lysates from these cells were resolved by SDS-PAGE and immunoblotted with an anti-M_3 receptor antiserum. **B, C**. Cells as in **A** were labelled with [^{32}Pi] and subsequently challenged with acetylcholine (ACH) or clozapine N-oxide (CNO) for 5 min. Lysates from these cells were immunoprecipitated with the anti-M_3 receptor antiserum and resolved by SDS-

Molecular Pharmacology Fast Forward. Published on August 31, 2011 as DOI: 10.1124/mol.111.074674
This article has not been copyedited and formatted. The final version may differ from this version.

PAGE (**B**) or following limited tryptic digestion, 2-dimensional peptide mapping (**C**). The figures are representative of results produced in 4 independent experiments.

MOL #74674

Figure 9 Appropriate agonists modulate phosphorylation of specific residues in hM_3 receptor variants equivalently

Flp-In™ T-REx™ 293 cells harboring VSV-G-SNAP hM_3-R (**left**) or VSV-G-SNAP hM_3-RASSL (**right**) were uninduced (no dox) or induced to express these constructs by treatment with doxycycline (2 $ng.ml^{-1}$, 24h). Following addition of acetylcholine (Ach) or clozapine N-oxide (CNO) for 5 min cell lysates were generated and resolved by SDS-PAGE and immunoblotted with phospho-specific antibodies able to identify phospho-serine 412 (**A**) or phospho-serine 577 (**B**). Data are representative are results produced in 3 independent experiments.

Figure 10 The basis of selective interactions of clozapine N-oxide with hM_3 - RASSL

The proposed binding mode of clozapine N-oxide (pink) to hM_3-R (**A**) and to the hM_3-RASSL (**B**). Mutation of Y3.33 (hM_3-R) to C3.33 (hM_3-RASSL) allows clozapine N-oxide to move in the binding site and to interact with T5.42 (H-bond depicted as dotted line). Residues within the binding site predicted to play important roles are denoted both as their position in the primary sequence of hM_3-R and by their relative positions within transmembrane helices as described by Ballesteros and Weinstein (1995).

Molecular Pharmacology Fast Forward. Published on August 31, 2011 as DOI: 10.1124/mol.111.074674
This article has not been copyedited and formatted. The final version may differ from this version.

TABLES Table 1 Comparisons of ligand affinity/potency at hM_3-R and hM_3-RASSL constructs

	hM_3-R FlAsH	**hM_3-RASSL FlAsH**	**VSV-SNAP-hM_3-R**	**VSV-SNAP-hM_3-RASSL**
[^{3}H]QNB (K_D)	75 +/- 28 pM	7.9 +/- 2.2 nM	35 +/- 9 pM	1.4 +/- 0.04 nM
B_{max} (pmol/mg)	6.5 +/- 0.66	3.5 +/- 0.89	12.6 +/- 1.2	2.6 +/- 013
Atropine (K_i)	0.74 +/- 0.1 nM	47 +/-17 nM	0.74 +/- 0.2 nM	23 +/-1.4 nM
FRET (pEC_{50})	4.9 +/- 0.2 (Cch) >3.0 (CNO)	>3.0 (Cch) 5.1 +/- 0.4 (CNO)	Not applicable	Not applicable
[Ca^{2+}] (pEC_{50})	7.2 +/- 0.04 (Cch) 7.8 +/- 0.3 (Ach)	7.6 +/- 0.1 (CNO)	7.5 +/- 0.4 (Cch)	7.7 +/- 0.6 (CNO)
pERK1/2(pEC_{50})	Not determined	Not determined	7.9 +/- 0.3 (Ach) 6.9 +/- 0.1 (Cch) >4.0 (CNO)	7.6 +/- 0.4 (CNO) > 4.0 (Cch)
Internalization (pEC_{50})	Not applicable	Not applicable	4.8 +/- 0.16 (Cch)	6.2 +/- 0.15 (CNO)

Ach = acetylcholine, Cch = carbachol, CNO = clozapine N-oxide. All experiments were performed on stable Flp-In™ T-REx™ 293 cell lines able to express the noted construct upon addition of doxycycline. Data shown are the mean and SEM of 2-4 independent experiments performed in triplicate (see text and Figure Legends for full details). B_{max} values were obtained from cells induced to express the receptors with a maximally effective concentration of doxycycline.

Figure 1

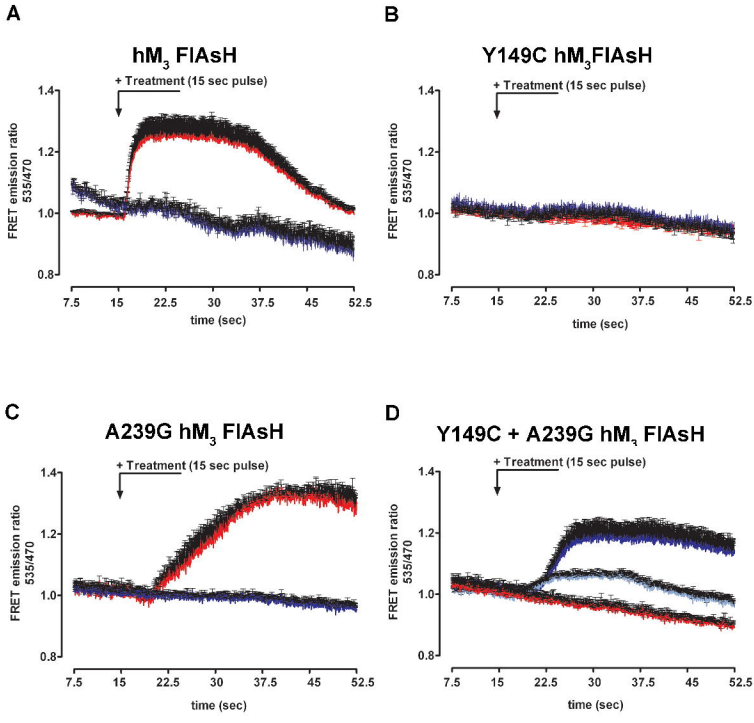
A
hM3 FlAsH
+ Treatment (15 sec pulse)
FRET emission ratio 535/470
time (sec)
B
Y149C hM3FlAsH
+ Treatment (15 sec pulse)
FRET emission ratio 535/470
time (sec)
C
A239G hM3 FlAsH
+ Treatment (15 sec pulse)
FRET emission ratio 535/470
time (sec)
D
Y149C + A239G hM3 FlAsH
+ Treatment (15 sec pulse)
FRET emission ratio 535/470
time (sec)

Figure 2

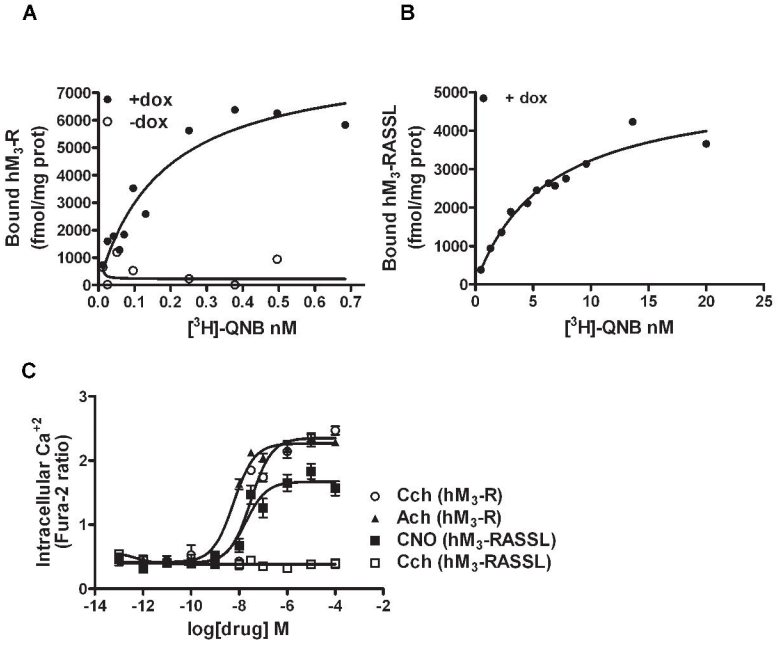
A
+dox
-dox
Bound hM3-R (fmol/mg prot)
[3H]-QNB nM
B
+ dox
Bound hM3-RASSL (fmol/mg prot)
[3H]-QNB nM
C
Intracellular Ca+2 (Fura-2 ratio)
log[drug] M
Cch (hM3-R)
Ach (hM3-R)
CNO (hM3-RASSL)
Cch (hM3-RASSL)

Figure 3

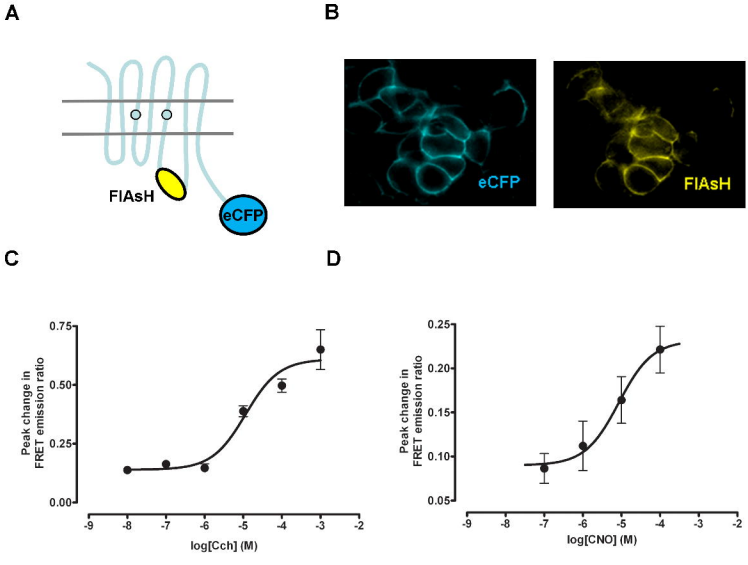
A
FlAsH
eCFP
B
eCFP
FlAsH
C
Peak change in FRET emission ratio
0.75
0.50
0.25
0.00
-9
-8
-7
-6
-5
-4
-3
-2
log[Cch] (M)
D
Peak change in FRET emission ratio
0.25
0.20
0.15
0.10
0.05
-9
-8
-7
-6
-5
-4
-3
-2
log[CNO] (M)

Figure 4

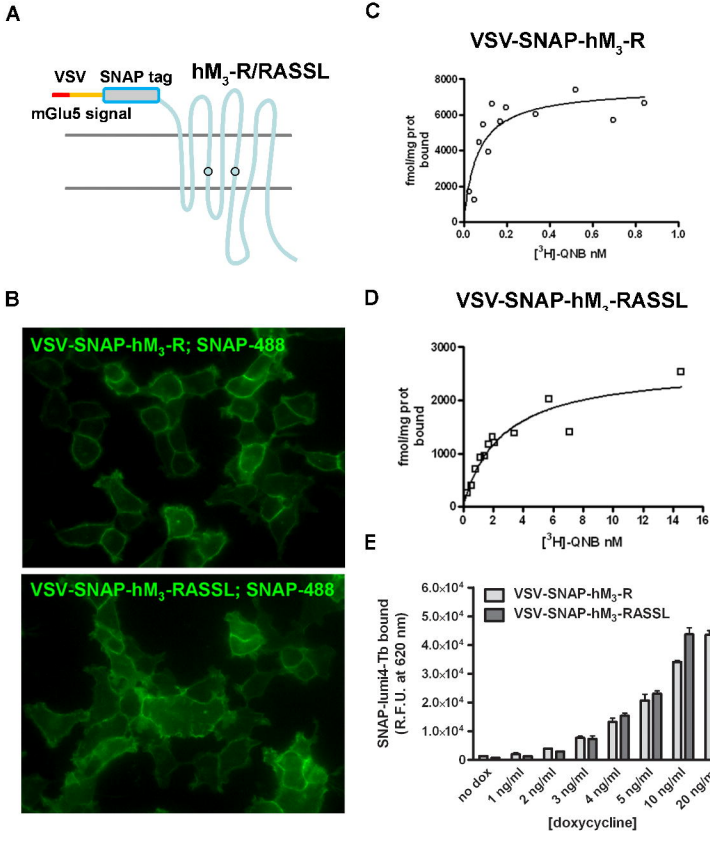
A
VSV
SNAP tag
mGlu5 signal
hM3-R/RASSL
B
VSV-SNAP-hM3-R; SNAP-488
VSV-SNAP-hM3-RASSL; SNAP-488
C
VSV-SNAP-hM3-R
fmol/mg prot bound
[3H]-QNB nM
D
VSV-SNAP-hM3-RASSL
fmol/mg prot bound
[3H]-QNB nM
E
SNAP-lumi4-Tb bound (R.F.U. at 620 nm)
VSV-SNAP-hM3-R
VSV-SNAP-hM3-RASSL
no dox
1 ng/ml
2 ng/ml
3 ng/ml
4 ng/ml
5 ng/ml
10 ng/ml
20 ng/ml
[doxycycline]

Figure 5

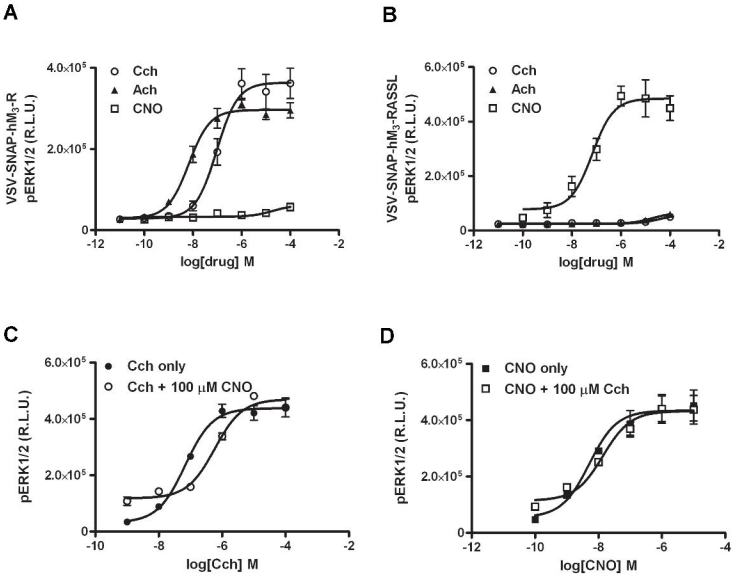
A
VSV-SNAP-hM3-R
pERK1/2 (R.L.U.)
4.0x10^5
2.0x10^5
0
Cch
Ach
CNO
-12
-10
-8
-6
-4
-2
log[drug] M
B
VSV-SNAP-hM3-RASSL
pERK1/2 (R.L.U.)
6.0x10^5
4.0x10^5
2.0x10^5
0
Cch
Ach
CNO
log[drug] M
C
pERK1/2 (R.L.U.)
6.0x10^5
4.0x10^5
2.0x10^5
0
Cch only
Cch + 100 μM CNO
log[Cch] M
D
pERK1/2 (R.L.U.)
6.0x10^5
4.0x10^5
2.0x10^5
0
CNO only
CNO + 100 μM Cch
log[CNO] M

Figure 6

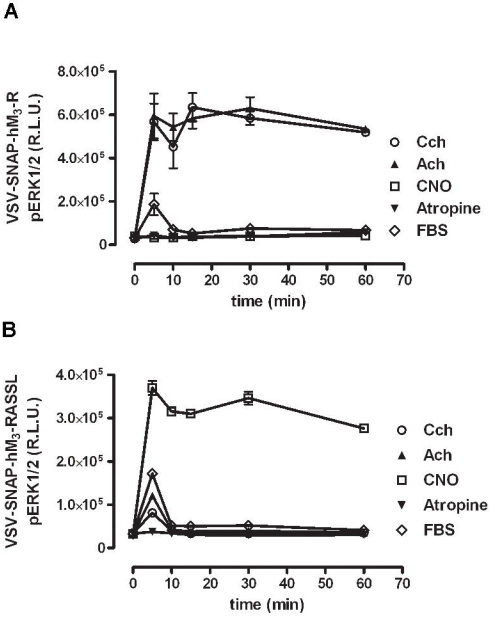
A
VSV-SNAP-hM3-R
pERK1/2 (R.L.U.)
8.0x10^5
6.0x10^5
4.0x10^5
2.0x10^5
0
0 10 20 30 40 50 60 70
time (min)
Cch
Ach
CNO
Atropine
FBS
B
VSV-SNAP-hM3-RASSL
pERK1/2 (R.L.U.)
4.0x10^5
3.0x10^5
2.0x10^5
1.0x10^5
0
0 10 20 30 40 50 60 70
time (min)
Cch
Ach
CNO
Atropine
FBS

Figure 7

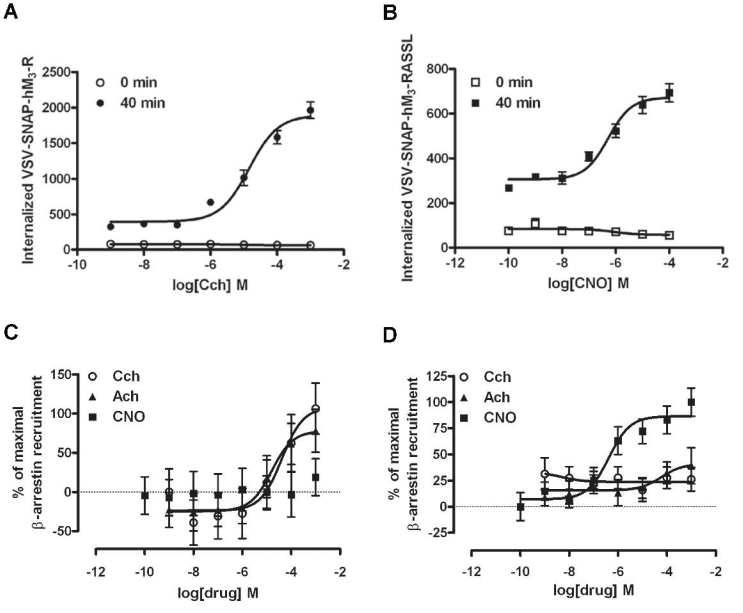
A
Internalized VSV-SNAP-hM3-R
0 min
40 min
log[Cch] M
B
Internalized VSV-SNAP-hM3-RASSL
0 min
40 min
log[CNO] M
C
% of maximal β-arrestin recruitment
Cch
Ach
CNO
log[drug] M
D
% of maximal β-arrestin recruitment
Cch
Ach
CNO
log[drug] M

Figure 8

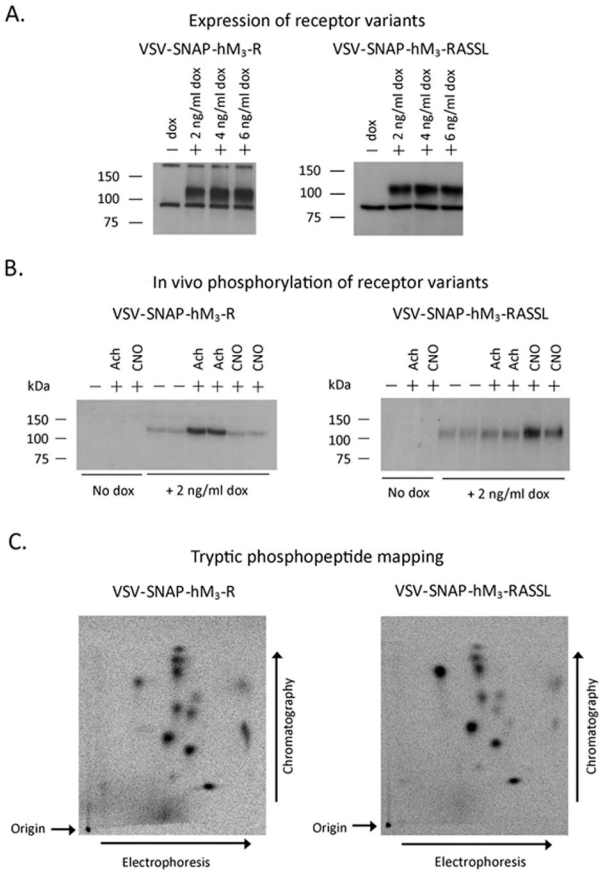
A.
Expression of receptor variants
VSV-SNAP-hM3-R
VSV-SNAP-hM3-RASSL
– dox
+ 2 ng/ml dox
+ 4 ng/ml dox
+ 6 ng/ml dox
150
100
75
B.
In vivo phosphorylation of receptor variants
VSV-SNAP-hM3-R
VSV-SNAP-hM3-RASSL
Ach
CNO
kDa
No dox
+ 2 ng/ml dox
C.
Tryptic phosphopeptide mapping
VSV-SNAP-hM3-R
VSV-SNAP-hM3-RASSL
Origin
Chromatography
Electrophoresis

Figure 9

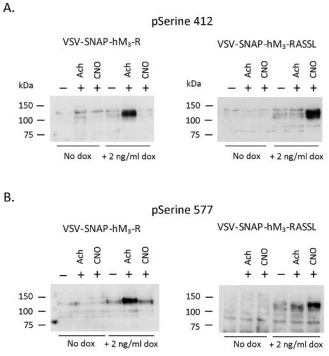
A.
pSerine 412
VSV-SNAP-hM3-R
VSV-SNAP-hM3-RASSL
kDa
Ach
CNO
150
100
75
No dox
+ 2 ng/ml dox
B.
pSerine 577
VSV-SNAP-hM3-R
VSV-SNAP-hM3-RASSL

Figure 10

A

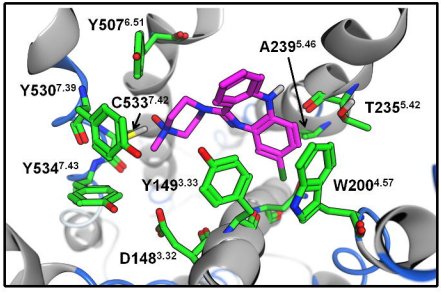
Y507$^{6.51}$
A239$^{5.46}$
Y530$^{7.39}$
C533$^{7.42}$
T235$^{5.42}$
Y534$^{7.43}$
Y149$^{3.33}$
W200$^{4.57}$
D148$^{3.32}$

B

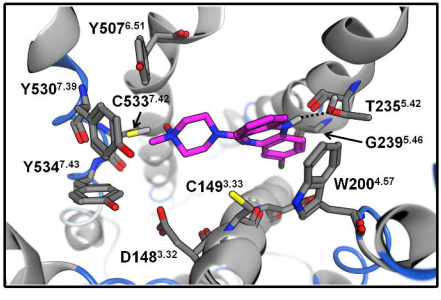
Y507$^{6.51}$
Y530$^{7.39}$
C533$^{7.42}$
T235$^{5.42}$
G239$^{5.46}$
Y534$^{7.43}$
C149$^{3.33}$
W200$^{4.57}$
D148$^{3.32}$